

# Characterization of self-healing polymers under simulated space environment

*L. Pernigoni<sup>1†</sup>, U. Lafont<sup>2</sup>, A. M. Grande<sup>1</sup>*

<sup>1</sup> *Department of Aerospace Science and Technology, Politecnico di Milano  
Via La Masa 34, 20156 Milan, Italy*

<sup>2</sup> *European Space Research and Technology Centre, European Space Agency  
Keplerlaan 1, PO Box 299, 2200 AG Noordwijk, The Netherlands*

*laura.pernigoni@polimi.it – Ugo.Lafont@esa.int – antoniomattia.grande@polimi.it*

<sup>†</sup> Corresponding Author

## Abstract

Self-healing inflatable structures are becoming increasingly appealing for space applications as combining their high packing efficiency and light weight with autonomous damage recovery would result in higher safety and reliability and lower costs. Nevertheless, a deeper knowledge of the effects of space environment on self-healing materials is needed.

In this work self-healing polymers are characterised before and after space conditioning to determine how space environment can affect their properties. It is observed that some factors significantly modify part of their properties, and the obtained results can help with the determination of actual behaviour and lifetime of these materials in space.

## 1. Introduction

Due to recent advances in space technologies, extended human missions on the Moon and Mars are likely to take place soon. The consequently related issue of prolonged exposure of crewmembers and devices to the threats of space environment will lead to stricter requirements on the spacecraft reliability, functionality, safety, and autonomy. As traditional architectures are typically unable to satisfactorily meet all these requirements, new materials and technologies must be considered to ensure long-term survival of space structures in outer space. In this context, self-healing materials have gained visibility as they can give increased reliability and safety and reduced maintenance costs of a spacecraft [1,2]. Implementing a self-healing mechanism into a design, after being damaged the material would be able to restore its main functionality partially or fully with low to no external intervention, and to almost immediately fix ruptures [3]. Nevertheless, little information regarding the effects of the combined environmental factors in space on self-healing materials is currently available, and a deeper knowledge of this topic is necessary to assess the applicability of these materials to space missions.

The objective of this work is hence to experimentally quantify the effects of space environment on physical, chemical, and mechanical properties of a set of self-healing polymers candidate for applications in flexible space structures such as habitats, space suits and gossamer devices. These materials are analysed before and after exposure to space environment simulated through the ESA ESTEC lab facilities in the Netherlands to determine how they respond to space conditioning. Gamma irradiation, outgassing, UV tests are performed, and rheological, thermal, spectroscopic characterisations are considered to understand their effects on the analysed polymers.

## 2. Materials and methods

### 2.1 Self-healing polymers

#### 2.1.1 Poly-urea urethanes

Four polyurea-urethanes (PUUs) with a fixed amount of disulphide linkages (dynamic covalent bonds) but variable crosslinking density are considered. They have a density of  $1 \text{ g/cm}^3$  and are obtained from different combinations of trifunctional and difunctional isocyanate-terminated pre-polymers PU 6000 and PU 4000 (Table 1), organised into networks connected by aromatic disulphides linkages and containing urea related H-bonds [4]. These pre-polymers can be synthesized through interaction of poly(propylene glycol) (PPG) and isophorone diisocyanate (IPDI) in the presence of the dibutyltin dilaurate (DBTDL) catalyst [5].

Table 1: Formulation of the analysed PUUs [4]

Polymer	Composition [wt%]		
	PU 6000	PU 4000	Linker
PUU 100	93.8	0	6.2
PUU 90	84.4	9.4	6.2
PUU 80	75.1	18.7	6.2
PUU 70	65.7	28.1	6.2

#### 2.1.2 Surlyn® 8940

Surlyn® 8940 is an intrinsic self-healing EMAA-based ionomer developed by DuPont, in which 30% of its MAA groups are neutralized with sodium ions. It has a density of  $0.95 \text{ g/cm}^3$  and is a thermoplastic polymer with a melting temperature of  $94 \text{ }^\circ\text{C}$  [6].

### 2.2 Samples preparation

The samples for the different baseline characterization tests are obtained from initial slabs or disks of material. The procedure followed for the manufacturing of the latter varies according to the considered polymer. As concerns the PUUs, 2 mm-thick slabs were already available.

For Surlyn® 8940, circular samples with thicknesses of approximately 0.7 mm and 0.8 mm, and initial diameters of 20 mm and 25 mm are obtained by compression of available ionomeric pellets (Fig. 1a) through a manual hot press pre-heated at around  $140 \text{ }^\circ\text{C}$ , and then left to cool at room temperature. A slab with 30x70 mm approximate size and 1 mm approximate thickness is also fabricated following the same procedure (Fig. 1b).



(a) Pellets



(b) Final slab

Figure 1: Surlyn® slab manufacturing

For the rheology, circular samples with a diameter of 25 mm are obtained from each slab or disk and are also used in the Attenuated Total Reflection Fourier Transform infrared (ATR FTIR) characterization. For the remaining DSC and TGA analyses, small samples with weights in the order of milligrams are taken from the starting material.

In the attempt of minimizing the effects of humidity on their properties, all the samples are degassed for 15 hours in vacuum at room temperature and subsequently kept in a desiccator with silica gel before undergoing each test.

## 2.3 Space conditioning tests

### 2.3.1 Outgassing screening test

An outgassing screening test is performed on the PUUs and on Surlyn® with the aim of determining their mass loss due to vacuum conditioning at high temperature and assessing the risk of contamination of sensitive surfaces (e.g.: mirrors, optical components) related to the use of these polymers in space. The tests are conducted in the  $\mu$ VCM facility of the TEC-QEE laboratory at ESA ESTEC (Fig. 2), following the ESA standards ECSS-Q-ST-70-02C and ECSS-Q-ST-70-05-C.

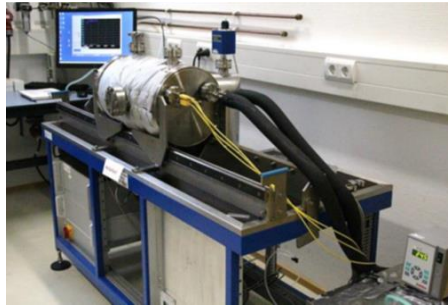


Figure 2: ESTEC  $\mu$ VCM facility

Three samples weighing between 100 and 300 mg are cut from each material and inserted into cups placed in a holder (Fig. 3) alongside empty cups used as reference blanks. Collector plates are also prepared for collection and analysis of material deposits condensed on them after outgassing.

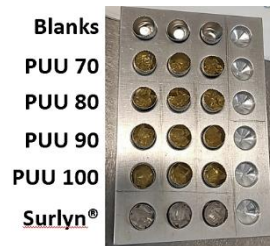


Figure 3: Sample holder for outgassing test

Before undergoing the outgassing test, the samples holder is inserted into a conditioning chamber for 24 hours at  $22 \pm 3$  °C and  $55 \pm 10\%$  relative humidity. The cups, the samples after the pre-test conditioning and the collector plates are weighted before starting the test.

The outgassing test lasts 24 hours, during which the samples are subjected to a temperature of 125 °C and pressures below  $10^{-5}$  mbar. The possible condensable material resulting from the treatment is collected on the collector plates kept at 25 °C. The samples subsequently undergo post-test conditioning for 24 hours at the same temperature and humidity used in the pre-test conditioning. Their masses right after outgassing and after the post-test conditioning are measured alongside those of the collector plates.

The main parameters considered for the evaluation of the outgassing performance of each material are the collected volatile condensable material (CVCM) and the recovered mass loss (RML), defined in this way:

$$\begin{cases} CVCM = \frac{W_g - W_p}{W_m} \times 100 \\ RML = \frac{W_0 - W_r}{W_m} \times 100 \end{cases} \quad (1)$$

$W_0$  and  $W_r$  are the sum of the mass of the sample and of the dedicated cup respectively right before outgassing and after outgassing and post-test conditioning.  $W_p$  and  $W_g$  are the initial and final masses of the collector plates, and  $W_m = W_0 - W_c$  is the initial specimen mass, where  $W_c$  is the mass of the dedicated cup. As a general guideline from the ECSS-Q-ST-70-02C standard, to be approved for use in space the materials should have  $RML < 1\%$  and

CVCM<0.1%. The average values of these quantities are here considered. If these requirements are not met, a possible solution is to perform a bakeout of the materials and test them again.

### 2.3.2 ESTEC Co60 irradiation tests

A set of irradiation tests is performed with the Co60 facility at ESA ESTEC (Fig. 4) on the materials. Two batches of circular neat samples with a diameter of approximately 25 mm are irradiated with a total ionizing dose in silicon of 100 and 500 krad respectively. Each batch is inserted into a sealable bag in which air is replaced with nitrogen to obtain a dry atmosphere and ideally remove the effect of humidity on the materials. The environmental conditions during irradiation are indicated in Table 2.



Figure 4: Co60 facility at ESTEC

Table 2: Environmental conditions during irradiation

	Temperature [°C]	Pressure [kPa]	Rel. humidity [%]
<b>Minimum</b>	23	100.31	43.9
<b>Maximum</b>	23.2	102.95	51.6

### 2.3.3 UV tests

The UV testing is performed in the CROSS1 facility at ESA ESTEC (Fig. 5) to evaluate possible effects of solar vacuum UV (VUV) radiation on the considered polymers. The facility consists of a high vacuum chamber operated below  $10^{-5}$  mbar, a sample plate assembly and a cold shroud cooled by liquid nitrogen. The UV irradiation set-up consists of an array of 4 halogen discharge lamps in open quartz which produces UV, visible and infrared radiation positioned outside the vacuum chamber and illuminating the sample plate at normal incidence.



Figure 5: CROSS1 facility at ESTEC

After fixing 20 mm diameter samples to a dedicated plate (Fig. 6), the system is sealed and UV irradiation is performed for 330 hours at a temperature of approximately 70 °C with an acceleration factor of 4.5 solar constants, corresponding to 1500 Equivalent Sun Hours (ESH).

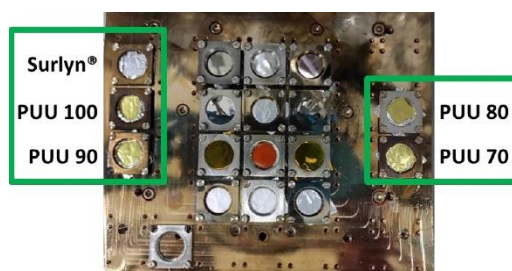


Figure 6: Plate in the CROSS1 facility

## 2.4 Materials characterisation

### 2.4.1 Rheology

The TA Instruments Discovery HR-2 rheometer with 25 mm aluminium parallel plate geometry and a Peltier plate for temperature control is used to perform shear tests on the PUUs and measure their storage and loss moduli  $G'$  and  $G''$ . A logarithmic frequency sweep is performed with 5 points per decade from 0.01 to 10 Hz at 25 °C, with 3 minutes soak time. The shear and initial compressive control force are set to 1% and 0.5 N respectively.

### 2.4.2 DSC and TGA measurements

DSC analysis is performed on all the materials with the Mettler Toledo DSC 822e module in nitrogen with 50 ml/min flow rate, using 40  $\mu$ l aluminium crucibles. For the PUUs a decreasing temperature ramp is initially performed at 20 °C/min from 25 °C to -110 °C. After an isothermal step the temperature is then increased up to 150 °C keeping the previous 20 °C/min ramp. The cycle is then repeated after moving back to -110 °C. The test parameters and followed experimental method remain unchanged for Surlyn®, except for the minimum temperature which is set to -140 °C. The chosen temperatures and repetition of the thermal cycle are related to the typically followed procedure for DSC analysis, in which the starting temperature is usually set at least 50 °C below the expected glass transition temperatures of the analysed materials.

TGA analysis is performed with the Mettler Toledo TGA/DSC 3+ device in nitrogen at 70 ml/min from 25 °C to 400 °C/min with a 20 °C/min ramp, using 70  $\mu$ l alumina crucibles. The main purpose of this analysis is to assess the temperature range within which the considered polymers remain stable.

### 2.4.3 ATR infrared spectroscopy

ATR FTIR characterization is performed on the materials under study to identify their chemical substances or functional groups by determining and looking at their spectra. The Bruker VERTEX 70v FTIR spectrometer with a germanium (Ge) crystal setup is used to acquire information in the wavenumber range from 650 to 4000  $\text{cm}^{-1}$  on the ATR spectra of the polymers. The signal gain, scanner velocity and background scans number are set to 8, 5 kHz and 64 respectively. The Ge crystal is cleaned right after each measurement, to prevent the just characterized sample from contaminating it and subsequently compromising the results of the following test.

## 3. Results and discussion

### 3.1 Outgassing

The results related to the mean outgassing parameters are listed in Table 3. PUU 90 and Surlyn® comply with the RML < 1% and CVCM < 0.1% acceptance limits, while the remaining PUUs have average CVCM values above the 0.1% threshold. A possible solution to this would be to perform a bakeout of these polymers and then test them again. Bakeout indeed helps to remove residual, process and handling contaminants from the samples and might be

sufficient to reduce the CVCM data to acceptable values. Furthermore, the ECSS-Q-ST-70-02C standard also indicates that the corrective actions to be taken to comply with the general requirements can be relaxed if the location of the material is far away from the sensitive items and/or if the material is shielded. The second condition would likely apply to the here presented PUUs, as they could mainly be used to manufacture intermediate layers in multilayer configurations.

Table 3: Average values of the outgassing parameters

Material	CVCM [%]	RML [%]
PUU 70	0.19	0.57
PUU 80	0.14	0.45
PUU 90	0.09	0.47
PUU 100	0.12	0.48
Surlyn®	0.02	0.46

Visual inspection of the collector plates proves the presence of condensed material on them, which is more evident for the PUUs. The plates are also analysed with the Bruker VERTEX 70v spectrometer with a Zinc Selenide (ZnSe) crystal setup in transmission mode to obtain the IR spectrum of the condensed contaminants as required by the ECSS-Q-ST-70-05C standard. The transmittance scale is given only for reference, and the spectra positions are shifted for the sake of clarity.

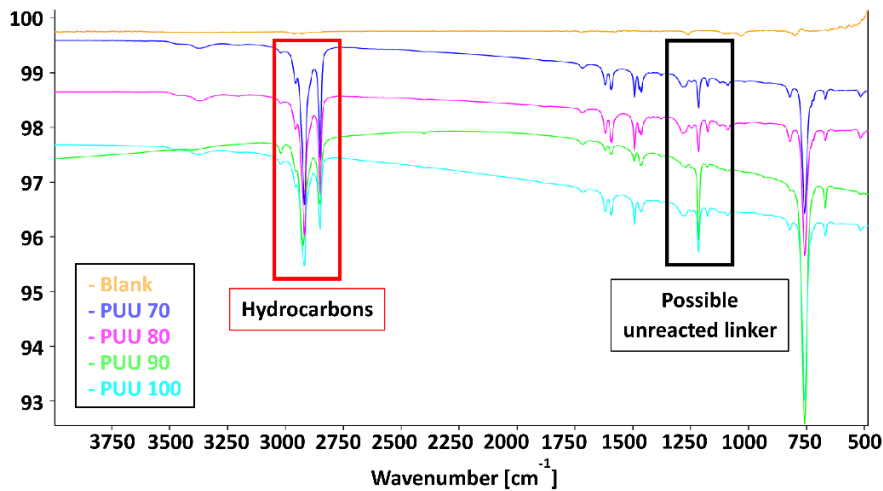


Figure 7: ATR IR spectrum of PUU condensates on the collector plates

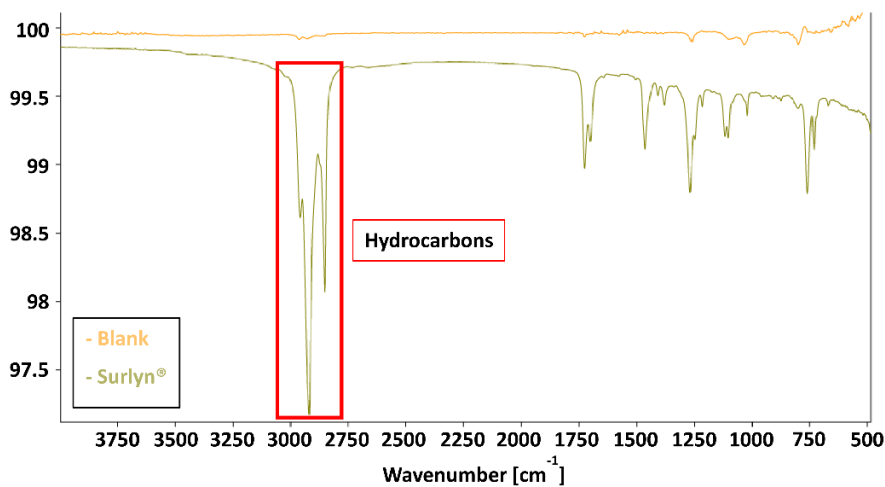


Figure 8: ATR IR spectrum of Surlyn® condensates on the collector plates

The ATR analysis indicates hydrocarbons as possible contaminants (alkanes functional group) for both the PUU family (Fig. 7) and Surlyn® (Fig. 8) in the region between 2750 and 3100  $\text{cm}^{-1}$ . Peaks in the PUUs fingerprint region are also observed close to 750  $\text{cm}^{-1}$  (assumed C-H bending vibration) and 1250  $\text{cm}^{-1}$  (possible C-N stretching). This second contribution might be due to the presence of unreacted linker (4-Aminophenyl disulfide) in the samples.

### 3.2 Materials characterisation

#### 3.2.1 Rheology

The PUU samples irradiated with the 100 krad and 500 krad doses are considered and compared to the corresponding blanks. Unfortunately, the rheological characterization of the UV-irradiated samples cannot be performed due to the damage imparted to the PUU 70, 80 and 90 samples and to the irregular structure of the PUU 100 sample, resulting from VUV conditioning (Fig. 9). A possible cause of this outcome might be an expansion of residual air between the supporting plate and the samples during the experiment, which could lead to the inflation, deformation, and subsequent rupture of the specimens. Future studies should indeed focus on rheological analysis after UV radiation, as this factor is likely to have relevant effects on the viscoelastic properties of the considered polymers.

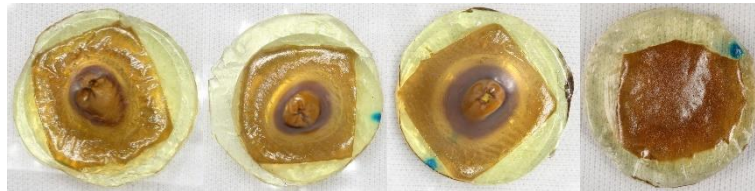


Figure 9: Samples after UV conditioning. From left to right: PUU 70, 80, 90 and 100

A slightly predominant elastic behaviour is observed ( $G' > G''$ ) in both the blank and irradiated batches, with an unclear pattern in the variation of the  $G'$  and  $G''$  values when moving from PUU 70 to PUU 100. A common behaviour with a stronger variation of  $G'$  and  $G''$  as the radiation dose increases would be instead expected, as the PUUs are very similar. A progressive decrease of the viscoelastic parameters after irradiation is observed only for PUU 80, which presents a very similar behaviour in the blank and 100 krad samples (Fig. 11). The opposite trend can be found in the PUU 70 case, which is however characterized by small  $G'$  and  $G''$  variations after irradiation, with the 100 krad and 500 krad having comparable properties (Fig. 10).

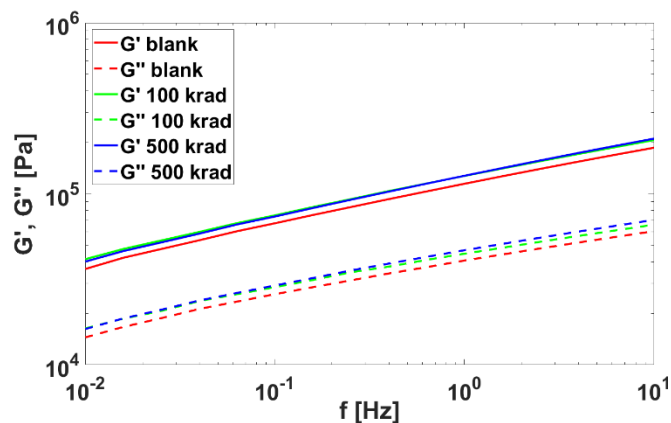


Figure 10: Blank-irradiated PUU 70 frequency sweep results comparison

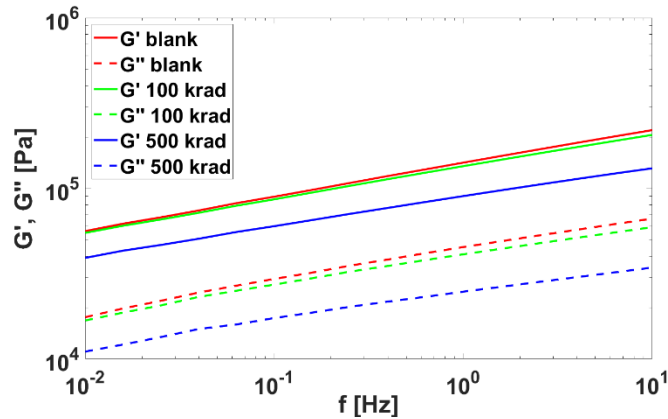


Figure 11: Blank-irradiated PUU 80 frequency sweep results comparison

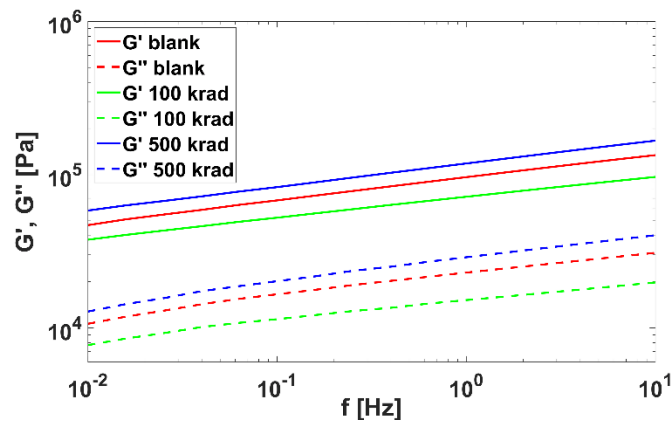


Figure 12: Blank-irradiated PUU 90 frequency sweep results comparison

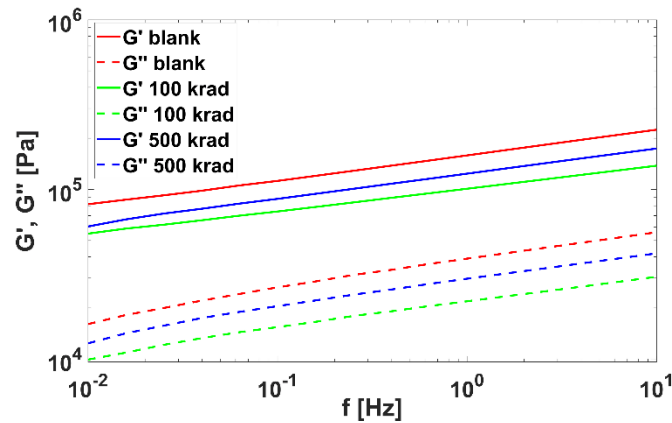


Figure 13: Blank-irradiated PUU 100 frequency sweep results comparison

The generally found high variability of the results might be partially due to the sensitivity of PUUs to humidity. The samples are degassed and stored in a desiccator in the attempt to minimize this effect, but residual moisture might still be present and partially affect the results. Further analysis and tests repetition after additional humidity removal procedures would hence be necessary to separate the effects of gamma radiation and moisture.

### 3.2.2 DSC and TGA measurements

The glass transition temperatures ( $T_g$ ) before and after gamma and UV irradiation are compared in Table 4. Surlyn<sup>®</sup> is not included as it does not possess a proper  $T_g$ . In the first DSC cycle, the blank ionomer exhibits two melting peaks (Fig. 14): the first one, around 61.7 °C, is related to melting of secondary crystallites and what is referred to as the passage from ordered to disordered state. A second peak is observed at 95 °C which indicates the primary crystal



phase melting. This peak is also present in the second cycle, differently from the first peak. The disappearance of the latter is caused by the long time needed to move back from disordered to ordered state of the ionic clusters. In short, following heating experienced during the first cycle, an ordered organization of the ionic clusters still needs to be restored in the sample. A crystallization peak of about 2 W/g at approximately 55 °C is also observed in both cycles.

Except for PUU 70, the 100 krad and 500 krad DSC results for the PUUs are basically identical, while they introduce slight  $T_g$  variations when compared to the blanks data. Interestingly, glass transition is not visible in the first cycle of the 100 krad PUU 70 sample (Fig. 15); this is probably due to experimental setup issues. An educated guess is that the time during which the sample is maintained at low temperature might have been not long enough to equilibrate the system before proceeding with the heating ramp. This phenomenon, related to the appearance and progressive right shift of something like an upside down "L", is also quite marked in the blank and UV Surlyn<sup>®</sup> curves (Fig. 14b) and in the UV-treated PUU 80 curve (Fig. 16). Aside from these considerations, no relevant variations are in general observed after space conditioning except for UV-treated Surlyn<sup>®</sup>: here, the crystallization peak is significantly flattened and the first and second melting peaks respectively shift leftwards and rightwards after conditioning.

Table 4:  $T_g$  values before and after space conditioning

Material	$T_g$ [°C]							
	Cycle I				Cycle II			
	Blank	100 krad	500 krad	UV	Blank	100 krad	500 krad	UV
PUU 70	-59.05	-	-58.64	-57.76	-58.99	-59.10	-58.63	-57.95
PUU 80	-58.28	-58.73	-57.92	-58.80	-58.74	-58.76	-57.94	-58.48
PUU 90	-58.12	-56.87	-58.45	-59.12	-57.88	-57.09	-58.07	-57.93
PUU 100	-58.59	-57.44	-56.99	-59.18	-58.63	-57.30	-57.12	-58.75

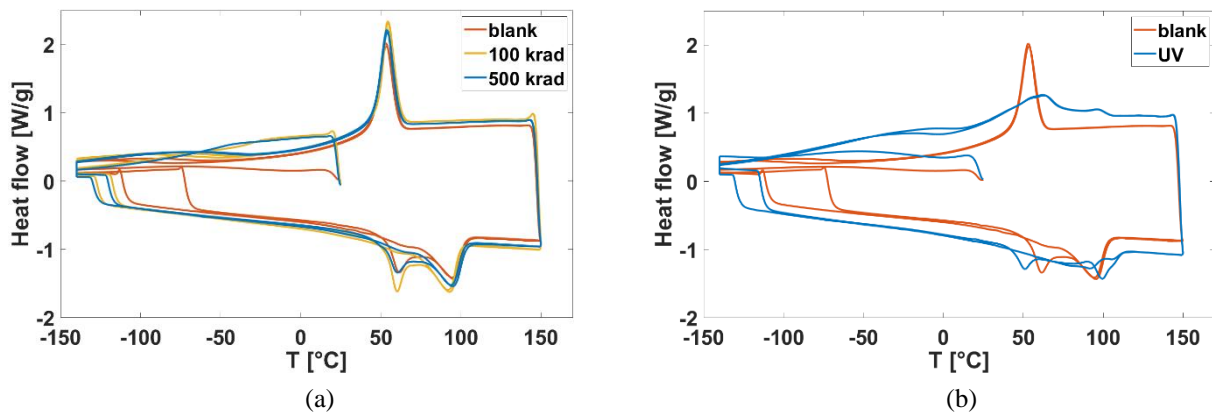


Figure 14: DSC results for blank Surlyn<sup>®</sup> compared with (a) irradiated and (b) UV-treated samples

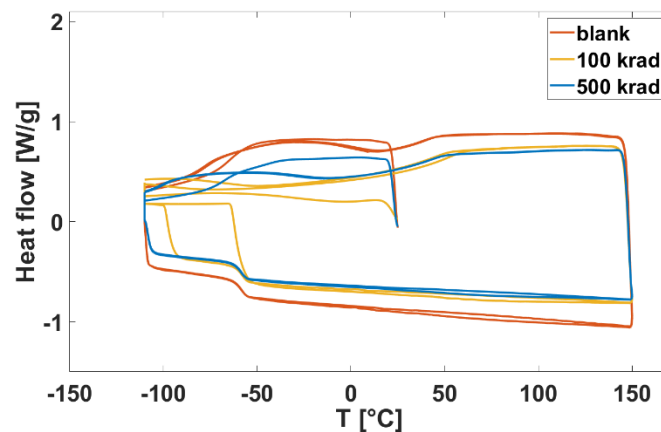


Figure 15: DSC results comparison of blank and irradiated PUU 70 samples

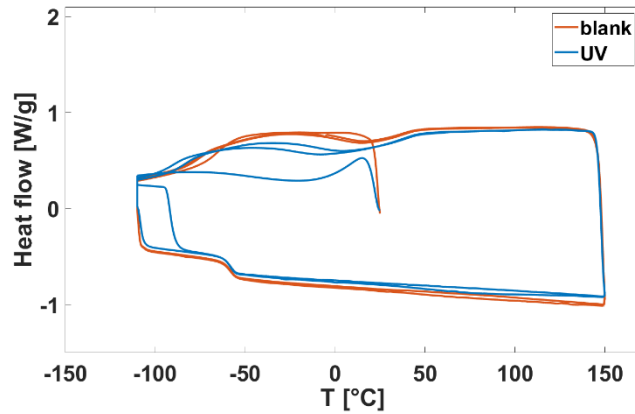


Figure 16: DSC results comparison of blank and UV-treated PUU 80 samples

For the TGA results, degradation onset temperature  $T_{5\%}$  determined at 5% of mass loss, degradation endset temperature  $T_{95\%}$  at 95% of mass loss, and maximum degradation temperature  $T_{max}$  determined at the peak of the first derivative of the TGA curve are listed in Table 5. Surlyn<sup>®</sup> is not included as its percentage mass remains above 96%, leading to no relevant thermal degradation temperatures. This polymer is hence more thermally stable than PUUs. In general, no relevant variations are observed in the TGA data after irradiation and UV treatment, as also shown by the examples in Fig. 17 and Fig. 18.

Table 5: TGA thermal degradation temperatures results

Material	Conditioning	$T_{5\%}$ [°C]	$T_{95\%}$ [°C]	$T_{max}$ [°C]
PUU 70	Blank	300.5	379.9	366.3
	500 krad	303.5	382.9	362.0
PUU 80	UV	304.7	381.2	366.0
	Blank	305.0	383.0	364.0
PUU 80	500 krad	302.9	381.6	366.0
	UV	304.5	383.2	361.0
PUU 90	Blank	302.4	381.9	363.7
	500 krad	303.3	380.5	358.3
PUU 90	UV	304.4	382.0	363.7
	Blank	303.8	381.9	363.7
PUU 100	500 krad	304.3	381.9	366.3
	UV	303.4	383.5	361.0

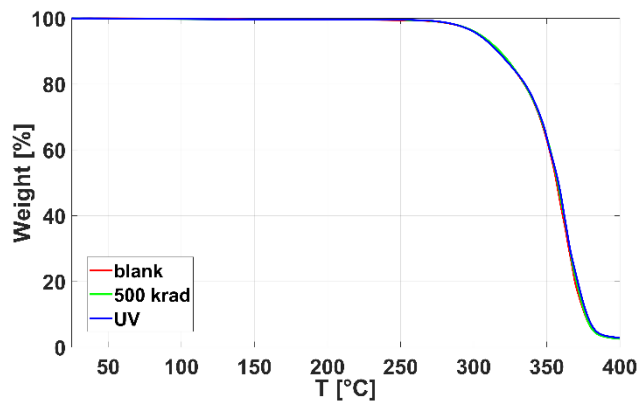


Figure 17: TGA curves comparison, PUU 100 example

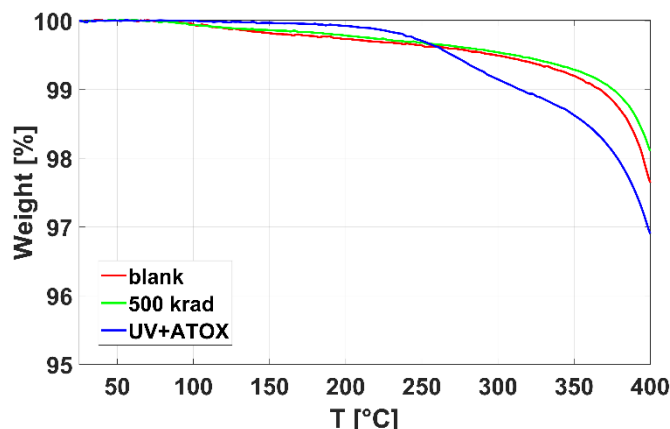


Figure 18: TGA curves comparison, Surlyn® example

After analysing the TGA results after the 500 krad dose it is decided not to characterize the 100 krad samples, as this is considered pointless. As a matter of fact, the absence of relevant changes in the TGA curves after exposure to the highest 500 krad dose is to assume that even smaller variations would be observed for weaker irradiation.

### 3.2.3 ATR infrared spectroscopy

The spectra of the blank PUUs are characterized by C-H stretching related to aliphatic hydrocarbons in the region between  $3000$  and  $2850\text{ cm}^{-1}$ , and a peak related to stretching of the O-H group is present at around  $3360\text{ cm}^{-1}$ . There is also a marked peak in the fingerprint region, at about  $1105\text{ cm}^{-1}$ , which is related to C=O stretching, while the shoulder at  $1660\text{ cm}^{-1}$  is attributed to urea. The spectra are basically the same for all the materials of this family, except for the wavenumber interval from  $2950\text{ cm}^{-1}$  to  $2800\text{ cm}^{-1}$ . As a matter of fact, PUU 90 and PUU 100 present a peak between  $2916$  and  $2917\text{ cm}^{-1}$  (Fig. 21 and Fig. 22), which is not observed in the other two PUU samples, and only PUU 90 is characterized by an additional peak at around  $2850\text{ cm}^{-1}$ . Nevertheless, these peaks are anyway still related to the functional group of aliphatic hydrocarbons, which is also in the spectrum of blank Surlyn®, in which C-H stretching is found at the two peaks at approximately  $2920$  and  $2850\text{ cm}^{-1}$ , and a C-H bending mode is related to the alkane methylene group at  $1465\text{ cm}^{-1}$ .

No relevant changes are observed after gamma irradiation, while UV conditioning has a relevant impact on the spectra of the analysed polymers. Focusing on the PUUs, some of the peaks related to the C-H stretching mode either disappear or shift. For example, considering PUU 70 a C-H stretch peak appears at approximately  $2920\text{ cm}^{-1}$ , and the alkane peak at about  $2898\text{ cm}^{-1}$  related to the blank PUU samples disappears (Fig. 19).

In the Surlyn® spectrum (Fig. 23), after UV irradiation a broad absorption band appears in the  $1650$ - $1590\text{ cm}^{-1}$  range which could be related to either COO<sup>-</sup> stretching or C=C stretching vibration. On the other hand, the peak present in the blank spectrum at  $1699.6\text{ cm}^{-1}$ , probably due to C=O stretching, disappears. A possible C=O stretch peak is instead observed after UV at  $1153\text{ cm}^{-1}$ , and possible phenol groups related to O-H bending are shifted to the right, from  $1399$  to  $1359\text{ cm}^{-1}$  and from  $1366$  to  $1327\text{ cm}^{-1}$  respectively.

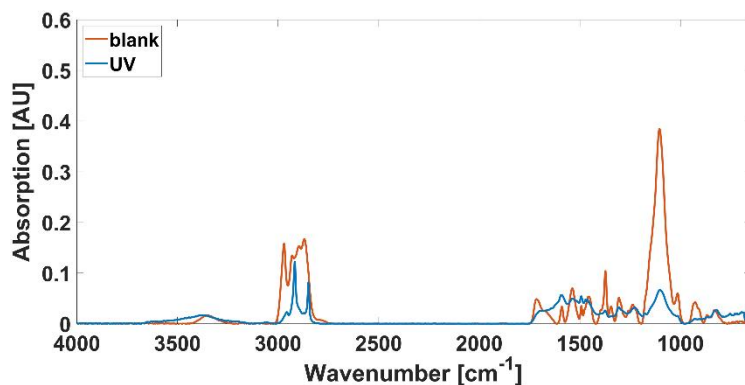


Figure 19: Comparison of IR spectra of blank and UV-treated PUU 70

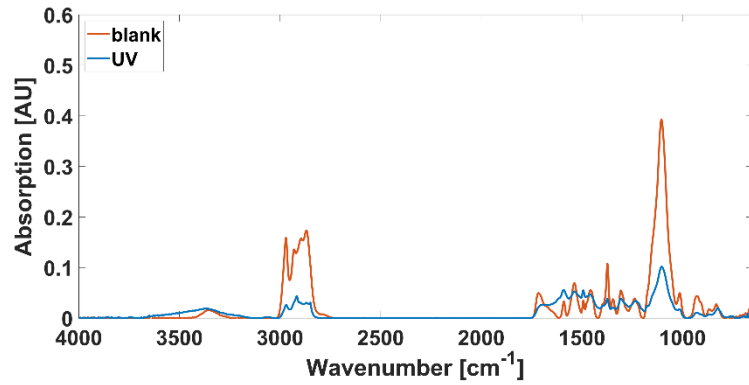


Figure 20: Comparison of IR spectra of blank and UV-treated PUU 80

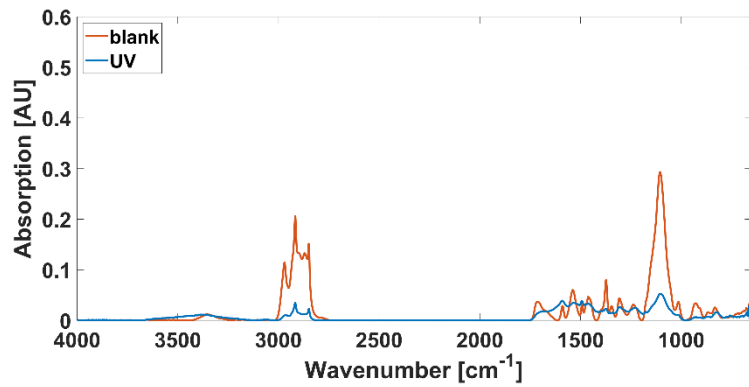


Figure 21: Comparison of IR spectra of blank and UV-treated PUU 90

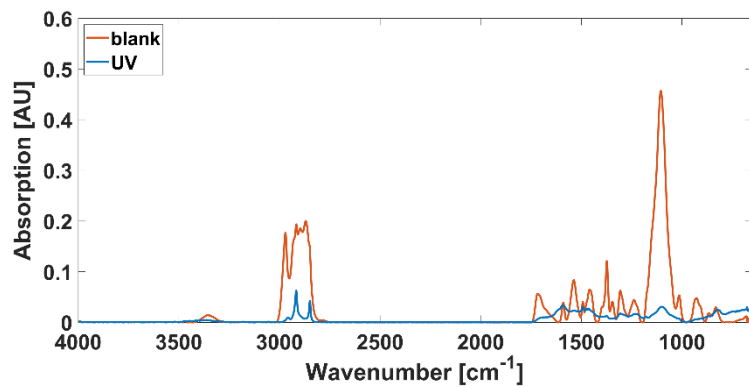
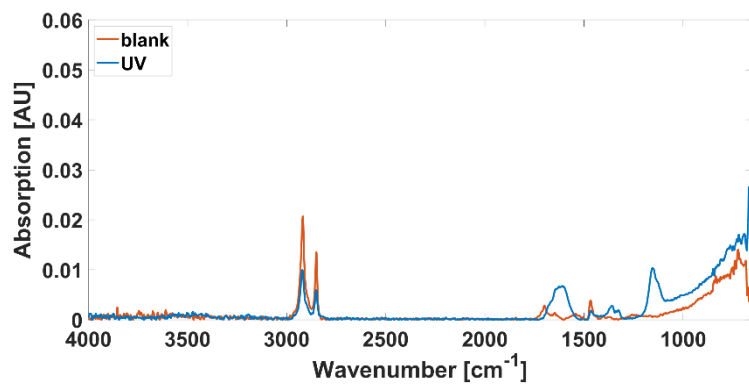


Figure 22: Comparison of IR spectra of blank and UV-treated PUU 100

Figure 23: Comparison of IR spectra of blank and UV-treated Surlyn<sup>®</sup>

## 4. Conclusions

This study analyses two types of self-healing polymers to assess their applicability to space structures. As regards the rheological properties of the PUUs, a large variability of the results is observed which might be related to high sensitivity to moisture. This requires additional tests to determine how and to what extent humidity affects these polymers, as this is an aspect of extreme importance for space applications. Furthermore, a rheological analysis of Surlyn® should be also performed. Nevertheless, the here presented shear tests would be destructive for the Surlyn® samples, as to obtain relevant information on its moduli the material would have to be heated above its melting temperature. As a result, it would stick to the rheometer plates, and the only way to remove it at the end of the test would be to scrape it off, leading to inevitable damage and the impossibility of perform multiple testing on the same sample. From these considerations, DMA tension or shear testing would be preferable for this polymer.

As concerns the effect on these materials of part of the environmental factors typical of space, interesting results related to the effects of solar UV radiation are found when analysing the ATR infrared spectra. In particular, strong modifications to the PUUs spectra suggests that the mechanical and self-healing properties of these polymers might be heavily affected by this environmental factor. For this reason, the future steps of this research must include repetition of UV irradiation experiments and subsequent mechanical and puncture tests on the materials, which were not possible in this research as the samples were damaged during conditioning. Differently from solar UV, gamma radiation does not seem to relevantly affect any of the here considered material properties; this is a positive outcome as it suggests high resistance of the polymers to this type of radiation. As a future step, the effect of proton and electron radiation must also be considered through additional experiments, which could not be performed during this research due to time and lab facilities availability limitations. It is suggested to perform tests through the ESA ESTEC Synergistic Temperature Accelerated Radiation (STAR) facility, which would expose the samples to intense ultraviolet radiation combined with electron and proton particle radiation, while in ultra-high vacuum, across an extreme range of temperatures ( $-150^{\circ}\text{C}$  to  $+350^{\circ}\text{C}$ ).

To conclude, this research shows that self-healing materials are promising for space applications, but there are still many improvements and additional characterization to be performed. Among the analysed materials, the PUUs seem the most suitable for space, but further understanding of the effects of humidity on them must be performed as this is a critical aspect especially for structures related to crewed missions, because an atmosphere and certain relative humidity levels would be required inside them. A useful approach for these applications would be to build a prototype of a multilayer configuration in which these materials would be inserted, and to experimentally analyse the changes in its healing performance at different humidity levels expected inside a space suit or a habitat. Possible solutions to control and limit the moisture content inside the materials could also be developed.

## Acknowledgements

This research was supported by ESA, contract No. 4000132669/20/NL/MH/ic.

## References

- [1] Naser, M.Z., A.I. Chehab. 2018. Materials and design concepts for space-resilient structures. *Prog. Aerosp. Sci.* 98:74–90.
- [2] Levchenko, I., K. Bazaka, T. Belmonte, M. Keidar, S. Xu. 2018. Advanced Materials for Next-Generation Spacecraft. *Adv. Mater.* 30:1–13.
- [3] ESA. 2006. Spacecraft, heal thyself. [http://www.esa.int/Enabling\\_Support/Preparing\\_for\\_the\\_Future/Discovery\\_and\\_Preparation/Spacecraft\\_heal\\_thyself](http://www.esa.int/Enabling_Support/Preparing_for_the_Future/Discovery_and_Preparation/Spacecraft_heal_thyself).
- [4] Grande, A.M., R. Martin, I. Odriozola, S. van der Zwaag, S.J. Garcia. 2017. Effect of the polymer structure on the viscoelastic and interfacial healing behaviour of poly(urea-urethane) networks containing aromatic disulphides. *Eur. Polym. J.* 97.
- [5] Rekondo, A., R. Martin, A. Ruiz de Luzuriaga, G. Cabañero, H.J. Grande, I. Odriozola. 2014. Catalyst-free room-temperature self-healing elastomers based on aromatic disulfide metathesis. *Mater. Horiz.* 1:237–240.
- [6] Grande, A.M., L. Castelnovo, L.D. Landro, C. Giacomuzzo, A. Francesconi, M.A. Rahman. 2013. Rate-dependent self-healing behavior of an ethylene-co-methacrylic acid ionomer under high-energy impact conditions. *J. Appl. Polym. Sci.* 130.